

## Quasi-Ordered Structure in Highly Cross-Linked Poly(acrylamide) Gels

D. Asnaghi,<sup>†</sup> M. Giglio,<sup>\*,†</sup> A. Bossi,<sup>‡</sup> and P. G. Righetti<sup>‡</sup>

Department of Physics and Istituto Nazionale di Fisica della Materia, University of Milan, Via Celoria 16, 20133 Milan, Italy, and Department of Agricultural and Industrial Biotechnologies, University of Verona, Strada Le Grazie, 37134 Verona, Italy

Received March 17, 1997; Revised Manuscript Received July 25, 1997<sup>®</sup>

**ABSTRACT:** By means of small-angle light scattering and turbidity measurements, we have studied the growth of highly cross-linked poly(acrylamide) gels, and show that they are endowed with a quasi-ordered structure. A peak at finite angle in the scattering profiles is observed, revealing the presence of a characteristic length scale in the range of a few micrometers. This length is larger for higher cross-linker content. The role of aggregation of the bis(acrylamide) cross-linker in determining the final structure of the gel is investigated by studying the polymerization of a pure bis(acrylamide) solution. The time evolution of the turbidity of the gels and the scattering profiles of the bis(acrylamide) solution suggest that cross-linker aggregation leads to two-phase separation. However, this process is arrested at a microscopic scale by the onset of gelation. The resulting structure is characterized by larger pores than in gels at standard cross-linker concentration, as can be seen from electrophoretic migration of large DNA fragments.

### 1. Introduction

In gel electrophoresis, molecules migrate through the interconnected pores of a gel under the effect of an applied electric field and are thereby sieved. For this application, networks with a uniform spatial distribution of pore (mesh) size are highly desirable. Poly(acrylamide) (PAAm) gels satisfying these requirements can easily be prepared and, for this reason, are widely used as migration media.<sup>1</sup>

In early experiments it has been shown that, at fixed total monomer concentration  $T$ , the gel pore size<sup>2,3</sup> and permeability<sup>4</sup> increase with the percentage  $C$  of the bis(acrylamide) cross-linker. In principle, this property could be exploited in order to manufacture gels with pore sizes changing over a wide range. However, already at  $C > 4$ –5% w/w,<sup>5</sup> PAAm gels are rather turbid, due to the presence of heterogeneities in the polymer concentration and thus in the refractive index. These heterogeneities have been ascribed to the occurrence of a microphase separation in the gelling polymer solution.<sup>6,7</sup> Recent results<sup>8</sup> support the idea that static inhomogeneities in the polymer concentration arise from freezing of critical fluctuations or microphase domains, present in the pregel polymer solution at the onset of gelation. The formation of bis(acrylamide) aggregates, favored by the fact that cross-linkers are more reactive than acrylamide monomers,<sup>9,10</sup> is also thought to induce inhomogeneities.<sup>5,9–13</sup>

A strong scattering at small angle from highly cross-linked PAAm gels has been first observed by Hecht *et al.*<sup>7</sup> The same feature has been reported in recent works<sup>14,15</sup> and explained by considering large clusters of cross-links distributed at random over the network.

In the present paper, we present small-angle light scattering data suggesting that the structural changes induced by the high cross-linker content can be exploited in order to obtain a quasi-regular network, characterized by a larger pore size. This result is confirmed by preliminary electrophoretic tests using DNA fragments.

We have studied gels at fixed total monomer concentration and at various percentages of the bis(acrylamide) cross-linker, during the copolymerization reaction. The measurements have been performed over an unusually wide range in wavevectors, spanning almost two decades, between  $6 \times 10^2 \text{ cm}^{-1}$  and  $5 \times 10^4 \text{ cm}^{-1}$ . For the first time, we observe a peak in the light scattered at nonzero wavevector, revealing the presence of quasi-periodical density fluctuations. This feature is typical of phase-separating liquid mixtures and has also been observed in a number of porous materials: porous glasses,<sup>16</sup> polymeric systems where gelation competes with segregation,<sup>17,18</sup> and microporous membranes.<sup>19</sup> The manufacturing of the materials listed above takes advantage of a spinodal decomposition process arrested by some solidification mechanism.

The time evolution of the turbidity, measured during the copolymerization process, strongly resembles that of a two-phase separating solution. However, the fact that turbidity eventually attains an asymptotic value reveals that the system is prevented from macroscopically separating by the onset of gelation.

It is well-known that the stability of a polymeric solution depends on the polymerization degree  $N$  of the solutes.<sup>20</sup> A polymer which is stable at low  $N$  in a given solvent, may be unstable in the same solvent at higher  $N$ . Thus, growth of a polymeric species in a solvent may lead to phase separation. In the present case, phase separation is induced by aggregation of the bis(acrylamide) monomers, as can be seen from light scattering measurements during cross-linking of a pure bis(acrylamide) solution.

### 2. Materials and Methods

**Sample Preparation.** Acrylamide (AAM), *N,N*-methylenebis(acrylamide) (BisAAM), *N,N,N,N*-tetramethylethylenediamine (TEMED), and ammonium persulfate were purchased from Bio-Rad Laboratories (Hercules, CA). Gels were prepared at room temperature (20 °C) from aqueous solutions with total monomer content  $T = 6\%$  g/mL (weight of AAM + BisAAM per volume solution) and with various cross-linkers concentrations  $C$ , namely 5%, 6%, 7%, 8%, 9%, 10%, and 15% (weight of BisAAM divided by weight of AAM + BisAAM). Polymerization was induced by a redox reaction, employing 0.45 mg/mL of ammonium persulfate and 0.5  $\mu\text{L/mL}$  of TEMED. In order

<sup>†</sup> University of Milan.

<sup>‡</sup> University of Verona.

<sup>®</sup> Abstract published in *Advance ACS Abstracts*, September 15, 1997.

to avoid an inhomogeneous distribution of the initiators, two aqueous solutions, the former containing the monomers plus TEMED and the latter ammonium persulfate, were prepared at twice the desired final concentration, filtered through a 0.22  $\mu\text{m}$  membrane filter and degassed with a water pump for 10 min. Then, equal volumes of the two solutions were rapidly mixed to start the polymerization, and the sample was immediately poured into the scattering cell.

**Small-Angle Light Scattering.** The small-angle light scattering apparatus employs a HeNe laser source and benefits from a custom made multielement sensor (a detailed description can be found in ref 17). A spatially filtered and collimated laser beam passes through a converging lens, then impinges on a cell with flat windows containing the sample, and is scattered. The scattered light is collected by a sensor lying in the back focal plane of the lens. The sensor consists of 31 concentric quarters of annuli with geometrically increasing radii and thicknesses. Thus, 31 transferred momenta  $q$  are simultaneously probed, their values depending on the cell-to-sensor distance and on the mean radii of the sensing elements.

The transmitted beam is focused onto a tiny hole in the center of the sensor and is detected by a photodiode placed behind. The sample turbidity can thus be determined. Intensity fluctuations of the incoming beam are monitored for data correction, and an initial sampling on nonreacting solutions is used for background subtraction.

Besides offering an unusually large range in wavevectors, this instrument also allows to perform measurements in rapid sequence. In particular, a rate of one sampling per second was used to follow the gelation kinetics. The measurements were performed at room temperature, at transferred momenta ranging from  $6 \times 10^2$  to  $5 \times 10^4 \text{ cm}^{-1}$ , i.e., at scattering angles between 0.38 and 32°.

**Electrophoretic Tests.** Gels used for DNA electrophoresis were prepared in an aqueous buffer (pH 8.3) at a concentration of 50 mM Tris-borate and 1 mM EDTA (Ethylenediaminetetraacetic acid), and were cast in the Bio Rad Mini-Protein II electrophoresis unit. The DNA fragments (Marker III, V, and VI from Boehringer, Mannheim, Germany) were added with bromophenol blue and loaded in pockets precast at the cathodic gel extremity. Electrophoresis was continued for 60 min at 120 V. After the gels were stained with ethidium bromide, the DNA bands were visualized by UV irradiation at 340 nm.

### 3. Experimental Results

The first set of measurements was performed 90 min after the beginning of polymerization, when the gelation process was completed. Very noisy intensity profiles were observed, unless the BisAAM content  $C$  was raised at least to 5% w/w.

In this case, unexpectedly, we found a peak at nonzero wavevector in the scattered intensity distributions. To our knowledge, this feature has never been observed before in the scattering from highly cross-linked gels, presumably because data are usually collected at larger wavevectors. In Figure 1 we plot the scattered distributions for gels at  $T = 6\%$  w/v and various cross-linkers content ( $C = 5\%, 6\%, 7\%, 8\%, 9\%, 10\%$ , and  $15\%$  w/w). The peak position depends weakly on the concentration of BisAAM, and the wavevector  $q_{\text{max}}$  corresponding to the maximum is smaller for higher  $C$ . In particular,  $q_{\text{max}}$  is nearly halved in going from  $C = 5\%$  to  $C = 15\%$ , while the maximum intensity increases by a factor of 5. Similarly, the beam attenuation over the 1 mm cell path grows, its values being 20.77%, 36.87%, 54.58%, 59.87%, 68.89%, 81.36%, and 84.54% for the curves shown. Obviously, a careful data correction would be mandatory in order to perform a quantitative analysis of the curves obtained in the presence of strong multiple scattering. However, the interpretation we present here is mainly based on qualitative features which are not too strongly affected by multiple scattering. In particu-

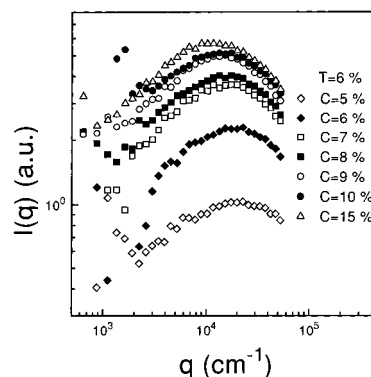


**Figure 1.** Scattered intensity distributions for gels with the following cross-linker content  $C$  (from bottom to top): 5%, 6%, 7%, 8%, 9%, 10%, 15%.

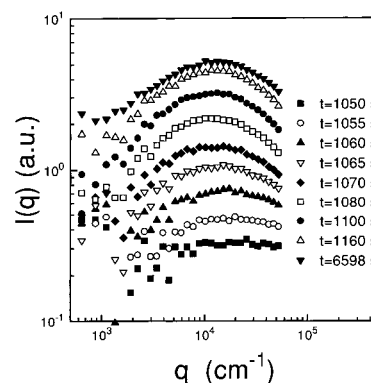


**Figure 2.** Time evolution of the scattering intensity distribution during polymerization for a gel with  $T = 6\%$  and  $C = 15\%$  ( $C_{\text{Bis}} = 0.9\%$ ). Time  $t = 0$  indicates the beginning of the polymerization process.

lar, it can be shown<sup>21</sup> that, even at the highest beam attenuation we measured, the position of the maximum in  $I(q)$  is not altered, the main effect of multiple scattering being a broadening of the peak.

The second set of measurements was performed as a function of time, during the course of polymerization. The reacting solutions were transparent for an initial time interval, and was accompanied by a rapid growth of turbidity. Figure 2 shows, as a function of  $q$ , the intensity scattered by a gel with  $T = 6\%$  w/v and  $C = 15\%$  w/w at various instants during polymerization. The first curve shown was collected roughly 15 min after the beginning of polymerization and is quite noisy. For earlier times, the scattering from the sample was so weak that reliable data could not be obtained. Later on, a maximum at nonzero wavevector developed, whose intensity increased by more than 1 order of magnitude in less than 2 min and whose position did not change noticeably. Eventually, the time evolution of  $I(q)$  slowed down, and it stopped entirely in about 90 min. The beam attenuation over the 1 mm cell path changed considerably during polymerization, varying between 13.00% and 79.97% from the first to the last curves plotted.

In order to determine the role of bis(acrylamide) aggregation on the properties of poly(acrylamide) gels, we studied a sample containing BisAAM only, at a concentration  $C_{\text{Bis}} = 0.9\%$  w/v (same concentration as in PAAm gel  $T = 6\%$  w/v and  $C = 15\%$  w/w). The intensity distributions, taken at various instants during polymerization, are shown in Figure 3. Similarly to the gel of Figure 2, the scattering profiles are peaked at a

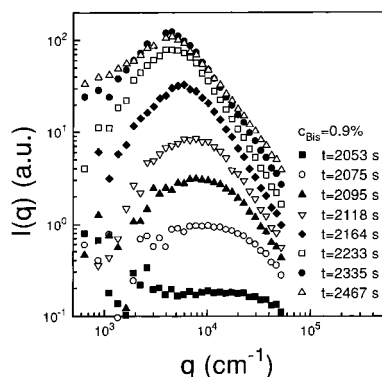


**Figure 3.** Time evolution of the scattering intensity distribution during polymerization for a solution of pure bis(acrylamide) with  $c_{\text{Bis}} = 0.9\%$ . Time  $t = 0$  indicates the beginning of the polymerization process.

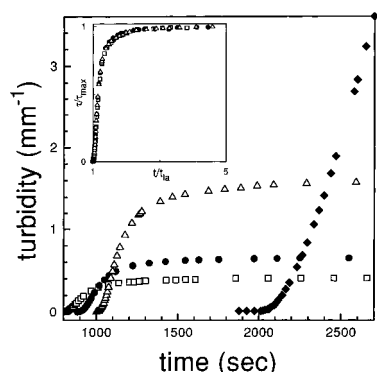


**Figure 4.** Time evolution of the turbidity during polymerization for gels with total monomer content  $T = 6\%$  and cross-linkers content  $C = 8\%$  (□),  $9\%$  (●),  $15\%$  (Δ). The turbidity is negligible for a time  $t_{\text{ia}}$  after which it increases noticeably, until it attains a plateau value  $\tau_{\text{max}}$ . In the inset, curves (□), (●), and (Δ) are scaled by plotting  $\tau/\tau_{\text{max}}$  vs  $t/t_{\text{ia}}$  (the following values of  $t_{\text{ia}}$  and  $\tau_{\text{max}}$  have been employed: 802 s and 0.408 (□); 889 s and 0.66 (●); 1001 s and 1.608 (Δ)). The growth of turbidity is also shown for a solution of pure bis(acrylamide) (◆,  $c_{\text{Bis}} = 0.9\%$ ).

finite wavevector. At variance with that gel, as time elapses, a displacement of the peak toward smaller wavevectors is evident. In particular, a  $q_{\text{max}}$  as small as  $5 \times 10^3 \text{ cm}^{-1}$  can be estimated. It can be noticed that the scattering profiles exhibit a power law decay at high  $q$ . From a nonlinear fit of the decay corresponding to  $t = 2233 \text{ s}$ , an exponent of  $-1.81 \pm 0.01$  was found. A similar behavior is observed in the high  $q$  range of the scattered intensity distributions from aggregating colloidal suspensions, where the noninteger exponent coincides with the aggregate fractal dimension.<sup>22</sup> In particular, a fractal dimension of roughly 1.8 is typical of aggregation processes controlled by particle diffusion (diffusion limited colloidal aggregation).

The observed increase in the opacity during polymerization at room temperature can be followed in detail in Figure 4, where the time evolution of the turbidity  $\tau$  is plotted for three gels at  $T = 6\%$  w/v and various  $C$ : 8%, 9%, and 15% w/w respectively. The turbidity is so weak as to be hardly detectable in the beginning, for a time  $t_{\text{ia}}$  on the order of 10–15 min. This time depends on cross-linkers concentration and is slightly shorter for lower  $C$ . Afterward, the turbidity grows rapidly for a few minutes, until it asymptotically reaches an equilibrium value  $\tau_{\text{max}}$ , which is larger for larger  $C$ . As can be seen in the inset, the shape of these three curves is such that they can be scaled onto a master curve, by plotting  $\tau/\tau_{\text{max}}$  vs  $t/t_{\text{ia}}$ .

**Table 1.** Relative Mobility  $R_f$  for DNA Fragments of Various Sizes (in bp) in Gels  $T = 6\%$  and  $C = 4\%$  and  $T = 6\%$  and  $C = 15\%$ , Respectively

base pairs (bp)	$R_f$ (%) in $T = 6\%$ and $C = 4\%$	$R_f$ (%) in $T = 6\%$ and $C = 15\%$
154	60	87.2
184	56.2	78.7
267	41.6	57.4
434	31	46.8
587	25	36
653	19.8	32
1033	12.7	27.6
1230	no migration	23.4
1766	no migration	18
2176	no migration	17

The time evolution of turbidity for the sample with  $c_{\text{Bis}} = 0.9\%$  w/v and no AAm is also plotted in Figure 4. As observed in the gels containing both AAm and BisAAm, there is a latency time  $t_{\text{ia}}$  after which  $\tau$  starts increasing. Moreover, the growth is as rapid as in the gel with  $T = 6\%$  w/v and  $C = 15\%$  w/w. However, the solution flocculates without attaining a jelly consistency, and at variance with the gel, no plateau region for  $\tau$  is observed during the experiment.

In order to have an estimate of the pore size, we studied the electrophoretic migration of DNA fragments ranging from 154 to 2167 base pairs (bp), in a standard PAAm gel with  $T = 6\%$  w/v and  $C = 4\%$  w/w and in the gel at high cross-linkers content used in Figure 2. The results are listed in Table 1, where the relative mobilities  $R_f$  are expressed as the ratio between the migration path of the fragments and the length of the gel. It is seen that the  $C = 15\%$  gel exhibits a larger pore size, since the mobility, which at low bp values is 45% larger than in the standard gel, becomes more than double for fragments above 1000 bp. It should be noticed that the three larger fragments can only be seen migrating in the  $C = 15\%$  gel; in the standard gel, they are probably trapped at the deposition site.

#### 4. Discussion

The major result of the present work is the observation of a maximum at nonzero wavevector in the light scattered by highly cross-linked poly(acrylamide) gels (see Figure 1). We would like to discuss here how the current model of the structure of these systems should change, on the basis of this new information.

In ref 15 (and similarly in ref 14) a monotonous decay of the scattered intensity distribution has been found, and the following formula proposed:

$$I(q) = \frac{I_L(0)}{1 + \xi^2 q^2} + I_G(0) \exp\left(-\frac{1}{3} R_g^2 q^2\right) \quad (1)$$

The scattering is thus written as the sum of a Lorentzian and a Gaussian term. The former accounts for the polymer–polymer correlations in a regular gel matrix and contains the correlation length  $\xi$ , while the latter arises from randomly distributed static inhomogeneities (with higher polymer concentration) of mean size  $R_g$ . By no means can this formula account for the depression in light scattered at very small angles, here observed. A schematic representation of the model described in ref 15 is drawn in Figure 5a, and the corresponding typical scattering profile is seen in Figure 5b.

In Figure 5c we have represented an alternative model for the gels microstructure and in Figure 5d the typical intensity distribution observed in the present

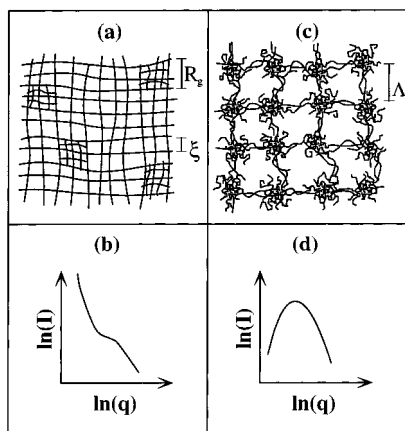


**Figure 5.** Structure of highly cross-linked gels as described in ref 15 (a) and the corresponding scattered intensity distribution (b). A schematic representation of the model here proposed is shown in part c, and the associated scattering profile is represented in part d.

work is displayed. The peculiar scattering profile is associated with the presence of quasi-periodical concentration fluctuations characterized by a preferred length scale  $\Lambda$ , related to the peak position

$$\Lambda = \frac{2\pi}{q_{\max}} \quad (2)$$

This characteristic length yields an estimate of the average pore size. As can be seen in Figures 1 and 2,  $q_{\max}$  ranges approximately from 1 to 2  $\mu\text{m}^{-1}$ , thus corresponding to a  $\Lambda$  of a few micrometers. It should be noticed that this value is much larger than the typical pore size for a PAAm gel at standard cross-linkers content, namely a few tens of nanometers.

Interestingly, an intensity distribution peaked at finite angle was observed a long time ago in small-angle neutron scattering from polystyrene networks with deuterated cross-links.<sup>23</sup> Since the most relevant contribution to neutron scattering is given by deuterated sites, this system allowed the characterization of the spatial distribution of cross-links, which was found to resemble an ordered lattice.

We have shown that most of the features typical of light scattering from highly cross-linked PAAm gels (Figure 2) are also exhibited by polymerizing cross-linkers solutions (Figure 3). Polymerization of a pure BisAAM solution spontaneously leads to the formation of branched polymers (chemical clusters), since these monomers are difunctional. Thus, in the present case, the main contribution to the scattering of gels arises from *clusters* of cross-linkers. These clusters are arranged in a quasi-ordered way, as indicated by the presence of a peak at  $q \neq 0$ . They grow in size during the polymerization process, as evidenced by the displacement of the peak toward smaller angles, as shown in Figure 3. They are fractal; i.e., their mass  $M$  scales with the radius  $R$  according to  $M \sim R^D$ , where  $D$  is a non integer exponent. This is revealed by the power law decay of the intensity distributions at high  $q$ ,  $I(q) \sim q^{-D}$ .

The presence of a peak at  $q \neq 0$ , the peak displacement as a function of time, and the noninteger exponent of the power law decay have also been observed during fractal aggregation of dense colloidal suspensions.<sup>24</sup> The two systems indeed exhibit strong similarities. It is known from the percolation theory (see for example refs 25 and 26) and from experimental work<sup>27</sup> that, during

polymerization of multifunctional monomers, fractal aggregates are formed before the onset of gelation. Both in colloidal suspensions and in polymeric gels, the quasi-ordered structure is associated with the high concentration of monomers.

Due to the aggregation of cross-linkers, branched polymers of increasing molecular weight grow in the solution. It is well-known that when the molecular weight and concentration of a polymer in a solvent are increased, phase separation can be induced.<sup>20</sup> The formation of BisAAM clusters causes a decrease in polymer-solvent compatibility, since a BisAAM-rich region is very hydrophobic. Furthermore, clustering implies an increase in the cross-links density. These two effects are known to give rise to phase separation during cross-linking copolymerization.<sup>6</sup>

We argue that the growth of bis(acrylamide)-rich branched polymers induces a phase instability, which leads to a sudden and rapid rise in the turbidity (Figure 4). Thus, the latency time  $t_{la}$  is the time that clusters take to grow so large and numerous as to induce phase separation of the solution. This time will depend on the aggregation rate and on the shape of the phase boundary. The increase of  $t_{la}$  with  $C$  at fixed  $T$  is probably due to a complex combination of these two elements.

We would like to point out that the existence of a latency time before the onset of phase separation has also been observed in PAAm gels grown in the presence of poly(ethylene glycol) (PEG).<sup>17</sup> In that system, phase separation is induced by polymerization of AAm, as PAAm and PEG are incompatible. A turbidity exhibiting a slow initial growth, a rapid increase, and a saturation has been recently found also in temperature quenched *N*-isopropylacrylamide gels and ascribed to a spinodal decomposition process.<sup>28</sup>

In the present case, the fact that turbidity eventually attains a finite value indicates that the phase separation process is arrested by the onset of gelation. Consistently, no slowing down is observed in the time evolution of  $\tau$  during the experiment on the nongelling BisAAM sample.

The scaling of the turbidity growth, shown in the inset of Figure 4, is rather peculiar. It appears that the turbidity curves reach their asymptotic value approximately after a time  $t_{\text{gel}} \approx 3t_{la}$ . This means that the time the system takes to gel scales with the time it takes to start separating.

We have argued that separation starts when the size and concentration of the bis(acrylamide)-rich clusters reach some critical values. We now assume that gelation takes place when these clusters are close-packed and fill the whole available volume. Then, the scaling of  $t_{\text{gel}}$  with  $t_{la}$  might be due to the fact that both separation and gelation are controlled by the same process, namely branching of BisAAM clusters.

Samples with higher bis(acrylamide) content present larger  $t_{la}$  (and thus larger  $t_{\text{gel}}$ ) and, at steady state, exhibit larger  $\Lambda$ , i.e. larger cluster size. This possibly means that, at higher  $C$ , a smaller number of clusters are formed, which can grow larger before coming into contact.

## 5. Conclusions

The possibility of manufacturing gels with a desired pore size is of great applicative interest in the electrokinetic separation of biological molecules.

Macropore formation in conjunction with the presence of a preformed polymer has been discussed in recent papers on PAAm gels<sup>17</sup> and agarose gels,<sup>29</sup> and a method for producing PAAm gels with templated pores was recently proposed.<sup>30</sup>

In this work, we have investigated highly cross-linked PAAm gels. It is known from pioneering works (see for example ref 2) that these gels are characterized by a pore size increasing with the cross-linker content. However, recent experiments<sup>14,15</sup> have given indication that inhomogeneities are randomly distributed over the matrix, making the gels inadequate for molecular sieving applications. At variance with these findings, we have shown by means of small-angle light scattering measurements that the gels exhibit a quasi-ordered structure, resulting from a competition between gelation and two-phase separation of the polymerizing solutions.

We have presented small-angle light scattering and turbidity data on poly(acrylamide) gels at various cross-linker content  $C$ , ranging from 5% to 15% by weight of the total monomer content  $T$  ( $T = 6\%$  w/v). Measurements have been performed as a function of time, during the copolymerization process of acrylamide and bis(acrylamide). For comparison, a pure bis(acrylamide) solution has also been studied with the same technique during cross-linking.

The light scattering profiles exhibit a peak at nonzero wavevector, revealing the presence of quasi-periodical density fluctuations. The system is characterized by a typical length in the range of a few micrometers, which is larger for higher cross-linker content.

The light scattering and turbidity data from the bis(acrylamide) solution show that the bis(acrylamide) monomers aggregate, thus causing a polymerization-induced instability. However, in the samples also containing AAm, further cross-linking induces an arrest of the phase-separation process to a microscopic extent. The resulting system is microsegregated.

Theoretical and simulation<sup>31</sup> work would be of great interest in order to have a deeper understanding of the complex phenomena involved in the formation of these gels.

**Acknowledgment.** M.G. and P.G.R. are supported by grants from Agenzia Spaziale Italiana (ASI, Roma) and by Consiglio Nazionale delle Ricerche (CNR, Roma) Comitato Tecnologico. P.G.R. additionally thanks the European Community for support (Human Genome

Project, Biomed 2, BMH4-CT96-1158).

## References and Notes

- (1) Chrambach, A.; Rodbard, D. *Science* **1971**, *171*, 440.
- (2) Fawcett, J. S.; Morris, C. J. O. R. *Sep. Sci.* **1966**, *1*, 9.
- (3) Righetti, P. G.; Brost, B. C. W.; Snyder, R. S. *J. Biochem. Biophys. Methods* **1981**, *4*, 347.
- (4) Weiss, N.; Van Vliet, T.; Silberberg, A. *J. Polym. Sci.: Polym. Phys. Ed.* **1981**, *19*, 1505.
- (5) Bansil, R.; Gupta, M. K. *Ferroelectrics* **1980**, *30*, 64.
- (6) Dusek, K. In *Polymer Networks*; Chomppff, A. J., Newman S., Eds.; Plenum: New York, 1971; pp 245–260.
- (7) Hecht, A. M.; Duplessix, R.; Geissler, E. *Macromolecules* **1985**, *18*, 2167.
- (8) Matsuo, E. S.; Orkisz, M.; Sun, S. T.; Li, Y.; Tanaka, T. *Macromolecules* **1994**, *27*, 6791.
- (9) Baselga, J.; Llorente, M. A.; Nieto, J. L.; Hernandez-Fuentes, I.; Pierola, I. F. *Eur. Polym. J.* **1988**, *24*, 161.
- (10) Suzuki, Y.; Nozaki, K.; Yamamoto, T.; Itoh, K.; Nishio, I. *J. Chem. Phys.* **1992**, *97*, 3808.
- (11) Richards, E. G.; Temple, C. J. *Nature* **1971**, *230*, 92.
- (12) Hsu, T.-P.; Ma, D. S.; Cohen, C. *Polymer* **1983**, *24*, 1273.
- (13) Hsu T. P.; Cohen, C. *Polymer* **1984**, *25*, 1419.
- (14) Mallam, S.; Horkay, F.; Hecht, A. M.; Rennie, A. R.; Geissler, E. *Macromolecules* **1991**, *24*, 543.
- (15) Cohen, Y.; Ramon, O.; Kopelman, I. J.; Mizrahi, S. *J. Polym. Sci., B: Polym. Phys.* **1992**, *30*, 1055.
- (16) Wiltzius, P.; Bates, F. S.; Dierker, S. B.; Wignall, G. D. *Phys. Rev. A* **1987**, *36*, 2991.
- (17) Asnaghi, D.; Giglio, M.; Bossi, A.; Righetti, P. G. *J. Chem. Phys.* **1995**, *102*, 9736.
- (18) Tromp, R. H.; Rennie, A. R.; Jones, R. A. L. *Macromolecules* **1995**, *28*, 4129.
- (19) Cipelletti, L.; Carpineti, M.; Giglio, M. *Langmuir* **1996**, *12*, 6446.
- (20) Flory, P. J. *Principles of Polymer Chemistry*; Cornell University Press: Ithaca, NY, 1953.
- (21) Cipelletti, L. Ph.D. Thesis, University of Milan, Milan, Italy, 1997.
- (22) Lin, M. Y.; Lindsay, H. M.; Weitz, D. A.; Ball, R. C.; Klein, R.; Meakin, P. *Proc. R. Soc. London, A* **1989**, *423*, 71.
- (23) Benoit, H.; Decker, D.; Duplessix, R.; Picot, C.; Rempp, P.; Cotton, J. P.; Farnoux, B.; Jannink, G.; Ober, R. *J. Polym. Sci., B: Polym. Phys.* **1976**, *14*, 2119.
- (24) Carpineti, M.; Giglio, M. *Phys. Rev. Lett.* **1992**, *68*, 3327.
- (25) Stauffer, D. *Introduction to percolation theory*; Taylor & Francis: London, 1985.
- (26) Adam, M.; Delsanti, M. *Contemp. Phys.* **1989**, *30*, 203.
- (27) Schosseler, F.; Daoud, M.; Leibler, L. *J. Phys. Fr.* **1990**, *51*, 2373.
- (28) Bansil, R.; Liao, G.; Falus, P. *Physica A* **1996**, *231*, 346.
- (29) Charlionet, R.; Levasseur, L.; Malandain, J. J. *Electrophoresis* **1996**, *17*, 58.
- (30) Rill, R. L.; Locke, B. R.; Liu, Y.; Dharia, J.; Van Winkle, D. *Electrophoresis* **1996**, *17*, 1304.
- (31) Moussaid, A.; *et al.* Paper in preparation.

MA970360F